# Bandwidth Utilization and Call Blocking Probability of OVSF Single-code Allocation with a Partial-loss Batch-arrival Model

陳瑞奇
國立中興大學資訊科學所
中州技術學院資訊管理系
rjchen@cs.nchu.edu.tw

陳文賢
國立中興大學資訊科學所
echen@cs.nchu.edu.tw

## 摘要

在第三代 WCDMA 無線網路中，一個 Node-B 基地台的正交可變展頻(OVSF)編碼數量是珍貴而有限的，過去已有許多 OVSF 編碼配置方法被提出來，並盡可能提供支援更多的用戶。本篇文章提出一個複數到達部分流失佇列模型，利用此模型來分析 OVSF 單碼配置系統，並可藉此計算出部份流失率及頻寬使用率，這兩個重要的效能參數分別代表用戶的服務品質及系統業者的收益。經由模擬比較顯示這個模型似乎可以用來分析前述系統，對於 WCDMA 無線網路建置時有所幫助。

**關鍵詞**：行動通訊，群組佇列，正交可變展頻編碼，頻寬使用率，部份流失率。

## Abstract

The orthogonal variable-spreading-factor (OVSF) codes in a Node-B of the 3G WCDMA network are limited and valuable. Many works have devised OVSF code-allocation schemes to support as many users as possible. This paper proposes a batch-arrival partial-loss queueing model to evaluate the performance of the OVSF single-code allocation system and obtains the expressions of partial loss probability and bandwidth utilization, both of which are two important performance measures for the system. They respectively denote the quality of service for subscribers and the profit of an operator. Simulation results show that the proposed model appear to work, which should be helpful for constructing WCDMA networks.

**Keywords**: Telecommunications, Batch Queue, OVSF code, Bandwidth Utilization, Partial Loss Probability.

## 1. Introduction

In the third generation (3G) Wideband-CDMA (WCDMA) networks, orthogonal variable spreading factor (OVSF) code transmission supports various wideband services with low or high data rates [1]. Both the forward and the reverse links in WCDMA can apply only one OVSF code, single code, to match a user-requested data rate [3-7]. The OVSF codes in a Node-B (the 3G base station) are valuable and limited, so 3G operators need to utilize them sufficiently. In recent years, several OVSF code-allocation schemes have been widely studied to support as many users as possible [1,7-13]. An OVSF code-allocation system can be viewed as a 3G cell (a Node-B may contains one or a few cells). Call blocking probability (CBP) and bandwidth utilization (BU) are two important performance measures for the OVSF code-allocation system, which respectively represent the quality of service (QoS) for subscribers and the profit of an operator. This paper proposes the batch-arrival partial-loss model $M[2^X]/M/c/c$ to evaluate the performance of an OVSF single-code allocation system and obtains the expressions of partial-loss CBP and BU. Operators can apply the measures to a utilization maximization problem that finds the optimal number of OVSF codes in a Node-B to gain the maximum profit with a specific QoS constraint. However, the proposed model should be useful for constructing WCDMA networks.

The remainder of this paper is organized as follows. The OVSF single code is described in Section 2. Section 3 illustrates the proposed model, while Section 4 conducts some important performance measures. Section 5 presents simulation results and verifies the theoretical analysis. Section 6 concludes this paper.

## 2. The OVSF Single Code

### 2.1 OVSF code generation

One spreading operation in WCDMA is the channelization that transforms each data symbol into a number of chips. The number of chips per data symbol is called spreading factor. The channelization codes are OVSF codes that preserve the orthogonality between channels of different rates. As shown in Fig. 1, a code tree recursively generates the codes based on a modified Walsh-Hadamard transformation [2]. $C_{ch,SF}^{k}$ denotes an OVSF code, where $SF$ is the spreading factor of a code, $k$ is the code number, and $1 \le k \le SF = 2^n$.

Variable spreading factors are used for the low and medium-high data rates. In the reverse link the spreading factors for data transmission range from 4 to 256, while in the forward link the factors vary from 4

to 512, with restrictions on the use of the factor 512. The maximum spreading factor $SF_{\max}$ usually equals the system capacity. Without loss of generality, the data rates described later are normalized by the basic data rate $R_b$ that denotes an OVSF code with $SF_{\max}$. Let all codes with the same spreading factor $SF$ be in the same level $log_2(SF)$ in the code tree. In other words, any code in the level $log_2(SF)$ is associated with the data rate $\frac{SF_{\max}}{SF} R_b$.

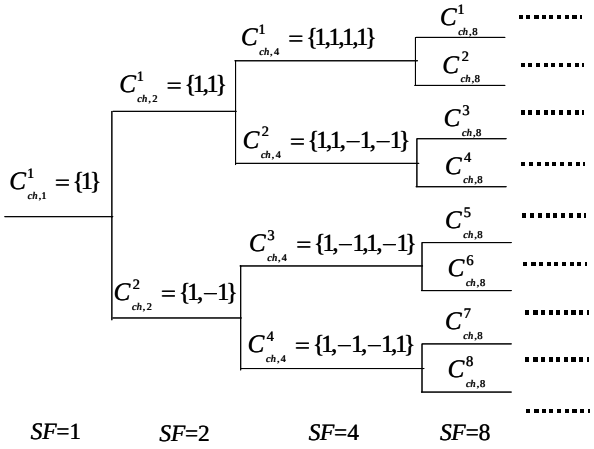


**Fig. 1. A code tree for generation of the OVSF codes**

## 2.2 Code-limited capacity test

Generally, a request rate $R_i$ for call $i$ can be expressed in a polynomial as $R_i = \sum_{j=0}^{n} r_j * 2^j$, where $r_j \in \{0,1\}$, $n = \log_2(SF_{\max})$, $1 \le R_i \le SF_{\max}$, and $R_i$ is the value of a multiplication of $R_b$. Before assigning a code, the cell has to check its available system capacity. There are two methods, interference-limited test and code-limited test, for measuring the system capacity. This paper adopts the code-limited test. And then the nonblocking condition can be defined in

$$\sum_{j=1}^{k-1} R_j + R_k \le SF_{\max} \cdot R_b. \quad (1)$$

Therefore, the system capacity is equal to $SF_{\max} \cdot R_b$ in a single cell. The cell may run out of the codes because the number of codes is limited. The call $i$ will be partially blocked if the above inequality is unsatisfied. Partial loss probability (PLP) denotes the partial-loss CBP of incoming call requests in a cell, expressed as the average number of partial blocked calls during a long enough period of time.

## 2.3 OVSF single code

One objective of the OVSF code allocation is to support as many users as possible. Using a single-code allocation scheme, a user equipment (UE) transmits its signal on only one channel with a variable data rate and requires only one RAKE receiver. A UE equipped with only one RAKE receiver can convey only a single-code rate $R_i$ with $\sum_{j=0}^{n} r_j \le 1$. Therefore, the call $i$ with $\sum_{j=0}^{n} r_j > 1$ will be assigned with an approximate and slightly higher single-code rate limited in one code, which can be expressed as

$$\xi(R_i) = 2^{\lfloor \log_2 (2*R_i - 1) \rfloor}. \quad (2)$$

# 3. M[$2^X$]/M/$c$/$c$ for the OVSF Single-code Allocation System

The number of OVSF codes with the maximum spreading factor $c = SF_{\max}$ usually denotes the system capacity in a cell. That is, the cell has in total $cR_b$ rate resources. The $c$ basic-rate codes can be explained as parallel multiple servers to serve $c$ channels simultaneously. A customer (call) can request multiple channels ranging from 1 to $2^K$ to meet its requirement. Hence, this case is treated as a batch (group; bulk) arrival. Let the customers arrive in groups following a Poisson process with the mean group-arrival rate $\lambda$, and the probability sequence $\{x_{2^k}\}$ govern arriving group size. Then $\lambda_{2^k}$ be the batch arrival rate with the group size of Poisson user stream $2^k$, where $\lambda_{2^k} = x_{2^k}\lambda$, $\sum_{k=0}^{K} x_{2^k} = 1$, $0 \le k \le K$, and $k, K \in \{0, N\}$. The rate $2^K$ is the admitted maximum request rate. The average group size $\overline{g} = \sum_{k=0}^{K} 2^k x_{2^k}$, where the probability density function of $x_{2^k}$ may be any countable distributions. Thus a new call assigned with $\xi(R_i) = 2^k R_b$ can be seen as a batch arrival with size $2^k$. On the other hand, a served call with $2^k R_b$ can be viewed as a continuous $2^k$ basic-rate codes released simultaneously. The service times (call holding times) are assumed to be independently exponentially distribution with the parameter $\mu$. Additionally, the system has no buffer (the queue length equals zero) so that the system is a partial loss system. If a new call finds that the available capacity in the corresponding cell cannot satisfy its rate requirement, it is just assigned the available rate (partially blocked). Hence, the single-code system can be modeled on the partial-loss batch-arrival model M[$2^X$]/M/$c$/$c$, the state-transition-rate diagram of which is depicted in Fig.2. The dotted lines in Fig. 2 denote other possible batch arrivals.

The equilibrium (steady-state) equations written below are run to obtain the steady-state probabilities $P_m$ of the model.

$$\lambda P_0 = \mu P_1, \text{ where } \lambda = \sum_{k=0}^{K} \lambda_{2^k}. \quad (3)$$

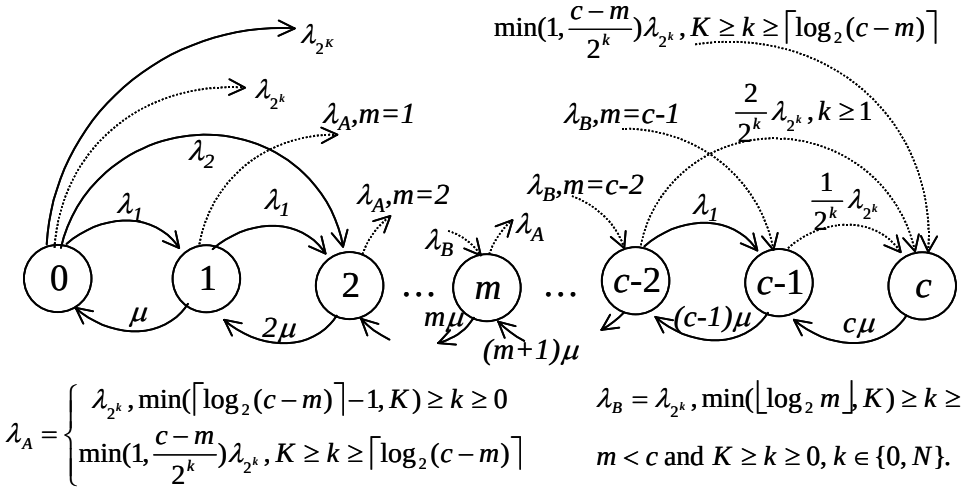


**Fig. 2. State-transition-rate diagram of M[$2^X$]/M/$c$/$c$ for the partial-loss OVSF single-code allocation system.**

$$\left( m\mu + \sum_{k=0}^{K} \min(\frac{c-m}{2^k},1)\lambda_{2^k} \right) P_m = \sum_{k=0}^{\min(\lfloor \log_2 m \rfloor, K)} \lambda_{2^k} P_{m-2^k} + (m+1)\mu P_{m+1}, \quad (4)$$

where $1 \le m \le c-1$.

$$c\mu P_c = \sum_{j=1}^{2^K} \sum_{k=\lceil \log_2 j \rceil}^{K} \min(\frac{j}{2^k},1)\lambda_{2^k} P_{c-j}, \quad (5)$$

which can be used for verification.

Reforming (3) and (4) yields

$$P_1 = P_0 \, \lambda/\mu, \text{ and} \quad (6)$$

$$P_{m+1} = \left[ \left( m\mu + \sum_{k=0}^{K} \min(\frac{c-m}{2^k},1)\lambda_{2^k} \right) P_m - \sum_{k=0}^{\min(\lfloor \log_2 m \rfloor, K)} \lambda_{2^k} P_{m-2^k} \right] \Big/ (m+1)\mu, \quad (7)$$

where $1 \le m \le c-1$.

However, the closed-form solution for $P_m$ is hard to express. Recursive programs cannot always solve the equations because of overabundant recursive levels for large $c$. Therefore, an iterative computer procedure can be used to derive the solution in the following.

Let $P_0^* = 1$; then $P_1^* = P_0^* (\lambda/\mu) = \lambda/\mu$. (8)

$$P_{m+1}^* = \left[ \left( m\mu + \sum_{k=0}^{K} \min(\frac{c-m}{2^k},1)\lambda_{2^k} \right) P_m^* - \sum_{k=0}^{\min(\lfloor \log_2 m \rfloor, K)} \lambda_{2^k} P_{m-2^k}^* \right] / (m+1)\mu, \quad (9)$$

where $1 \le m \le c-1$.

According to the normalizing condition $\sum_{i=0}^{c} P_i = 1$, the equilibrium probabilities of all states can be written as follows:

$$P_m = P_m^* \Big/ \sum_{i=0}^{c} P_i^*, \text{ where } 0 \le m \le c. \quad (10)$$

## 4. Performance Measures

With the equilibrium state probabilities, the PLP and BU can be derived forwardly. Now if a new single-code call with rate-$2^k$ finds that the available capacity in the corresponding cell cannot satisfy its rate requirement, then it is partially blocked. Hence the PLP of the proposed model can be written as

$$\alpha = \frac{1}{\lambda} \sum_{i=0}^{2^K-1} \sum_{k=\lceil \log_2(i+1) \rceil}^{K} \frac{2^k - i}{2^k} \lambda_{2^k} P_{c-i}, \quad (11)$$

where $c = SF_{\max}$, $K \ge 0$, and $\lambda = \sum_{k=0}^{K} \lambda_{2^k}$.

For example, let $K = 2$, then

$$\alpha = P_c + \frac{1/2\lambda_2 + 3/4\lambda_4}{\lambda_1+\lambda_2+\lambda_4} P_{c-1} + \frac{2/4\lambda_4}{\lambda_1+\lambda_2+\lambda_4} P_{c-2} + \frac{1/4\lambda_4}{\lambda_1+\lambda_2+\lambda_4} P_{c-3}. \quad (12)$$

In subsequence, the average number of customers (average system length; ASL) in the proposed model is

$$L = \sum_{i=0}^{c} i P_i, \quad (13)$$

which equals the mean number of busy servers in the model.

When the single-code allocation system is observed for a long period of time, the average BU can be expressed as

$$\beta = L / c. \quad (14)$$

Moreover, the average system waiting time (system delay) is shown as

$$W = 1/\mu. \quad (15)$$

In [14], the model $M^X$/M/$c$ calculates the traffic intensity by $\rho = \bar{g}\lambda / c\mu$, where a steady state

exists if $\rho < 1$. Nevertheless, the proposed model is a loss system and can apply $\rho > 1$.

## 5. Theoretical and Simulation Results

Some performance measures for the proposed model were evaluated for two cases in which the arriving group size has a discrete uniform distribution (DUNI) and a geometric distribution (GEOM). One can apply any countable distributions, e.g., constant, discrete uniform, and geometric distributions, for mapping the behavior of the arriving group size. Additionally, note that the *i*-th call requesting the rate $R_i$ will be assigned with the single-code rate $\xi(R_i)$. Of course, the system has offered load $\overline{g}\lambda/\mu$ and traffic intensity $\rho = \overline{g}\lambda/c\mu$.

### 5.1 Batch-arrival size in discrete uniform distribution (DUNI)

The PLP and BU were calculated with various values of $\rho$ ranging from 0.61 to 2.79, where $c$=256, $\mu$ = 0.00125, and $\lambda$ ranging from 0.03125 to 0.14375. Here the arriving group size was distributed with DUNI, where the maximum group size was 16 ($K$ = 4) and the average arriving group size $\overline{g}$ = 6.2, that is, $\xi(R_i)$ = 1, 2, 4, 8, or 16$R_b$ and $\lambda_1 = \lambda_2 = \lambda_4 = \lambda_8 = \lambda_{16} = \lambda/5$. Figure 3 shows the performance comparison between theoretical and simulation PLP and BU results, where the horizontal axis denotes the traffic intensity by $\rho = \overline{g}\lambda/c\mu$ and the vertical axis representing the PLP and BU ranges from 0.0 to 1.0. The theoretical PLP and BU are respectively shown as the solid lines with squares and circles, while the simulation PLP and BU are presented as the dotted lines with cross signs and plus signs. As indicated in Fig. 3, both the PLP and the BU increase with rising $\rho$. Figure 3 also show that the theoretical results are close to the simulation results. Apparently, the proposed model appears to work. Table 1 lists the numerical data of the comparison between the theoretical analysis and the simulation. The theoretical and simulation system delays, which are not shown in the table, were also compared. Their experimental values are also close to each other.

### 5.2 Batch-arrival size in geometric distribution (GEOM)

The arriving group size is herein assumed to have a GEOM distribution ($\lambda_1$: $\lambda_2$: $\lambda_4$: $\lambda_8$: $\lambda_{16}$ = 0.636409: 0.234122: 0.086129: 0.031685: 0.011655), where $K$ = 4, $\overline{g}$ = 1.889129, $\mu$ = 0.0025, and $\lambda$ ranges from 0.03 to 0.155. Surely, $\rho$ varies from 0.71 to 3.66. Table 2 compares the PLP and BU values of the theoretical analysis and simulation. The results present that the theoretical analysis has good approximate values as those the simulation does.

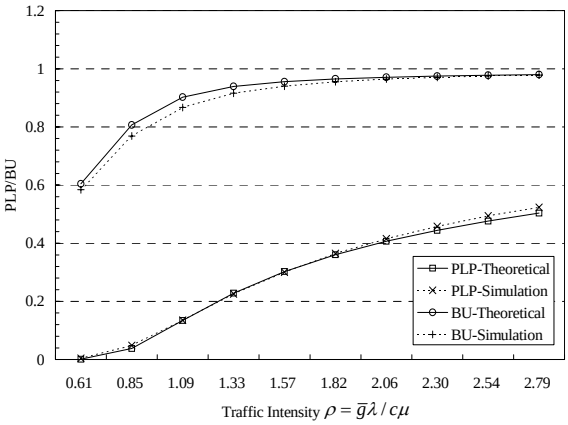


**Fig. 3. Performance comparison between theoretical and simulation PLP and BU results, where $c$=256, $K$ = 4, $\mu$ = 0.00125, and $\overline{g}$ = 6.2.**

**Table 1. Comparison for PLP and BU between theoretical (theo.) and simulation (simu.) results by DUNI group-size distribution, where $c$=256, $K$ = 4, $\mu$ = 0.00125, and $\overline{g}$ = 6.2**

| | PLP | | BU | | ASL | |
|---|---|---|---|---|---|---|
| $\rho$ | theo. ($\alpha$) | simu. | theo. ($\beta$) | simu. | theo. ($L$) | simu. |
| 0.61 | 0.0011 | 0.0043 | 0.6046 | 0.5841 | 154.8 | 149.4 |
| 0.85 | 0.0380 | 0.0488 | 0.8071 | 0.7689 | 206.6 | 196.7 |
| 1.09 | 0.1343 | 0.1351 | 0.9028 | 0.8670 | 231.1 | 221.8 |
| 1.33 | 0.2285 | 0.2258 | 0.9393 | 0.9161 | 240.5 | 234.4 |
| 1.57 | 0.3028 | 0.3007 | 0.9559 | 0.9404 | 244.7 | 240.6 |
| 1.82 | 0.3606 | 0.3646 | 0.9651 | 0.9553 | 247.1 | 244.4 |
| 2.06 | 0.4067 | 0.4153 | 0.9710 | 0.9646 | 248.6 | 246.8 |
| 2.30 | 0.4445 | 0.4580 | 0.9750 | 0.9706 | 249.6 | 248.3 |
| 2.54 | 0.4762 | 0.4942 | 0.9780 | 0.9754 | 250.4 | 249.5 |
| 2.79 | 0.5034 | 0.5238 | 0.9803 | 0.9785 | 250.9 | 250.3 |

**Table 2. Comparison for PLP and BU between theoretical (theo.) and simulation (simu.) results by GEOM group-size distribution, where $c$=32, $K$ = 4, $\mu$ = 0.0025, and $\overline{g}$ = 1.889129**

| | PLP | | BU | | ASL | |
|---|---|---|---|---|---|---|
| $\rho$ | theo. ($\alpha$) | simu. | theo. ($\beta$) | simu. | theo. ($L$) | simu. |
| 0.71 | 0.0424 | 0.0636 | 0.6430 | 0.6184 | 20.6 | 19.8 |
| 1.00 | 0.1174 | 0.1442 | 0.7887 | 0.7636 | 25.2 | 24.4 |
| 1.30 | 0.2097 | 0.2344 | 0.8651 | 0.8468 | 27.7 | 27.1 |
| 1.59 | 0.2969 | 0.3138 | 0.9056 | 0.8930 | 29.0 | 28.5 |
| 1.89 | 0.3720 | 0.3838 | 0.9289 | 0.9211 | 29.7 | 29.4 |
| 2.18 | 0.4349 | 0.4400 | 0.9435 | 0.9378 | 30.2 | 30.0 |
| 2.48 | 0.4874 | 0.4893 | 0.9533 | 0.9498 | 30.5 | 30.4 |
| 2.77 | 0.5316 | 0.5303 | 0.9604 | 0.9583 | 30.7 | 30.6 |
| 3.07 | 0.5691 | 0.5642 | 0.9656 | 0.9642 | 30.9 | 30.8 |
| 3.37 | 0.6012 | 0.5951 | 0.9696 | 0.9691 | 31.0 | 31.0 |
| 3.66 | 0.6290 | 0.6200 | 0.9728 | 0.9726 | 31.1 | 31.1 |

## 6. Conclusion

This study demonstrates the effectiveness of the batch-arrival partial-loss model $M[2^X]/M/c/c$ for analyzing the OVSF single-code allocation system. The simulation results agree with the predictions derived from the proposed model, indicating that the model successfully evaluates the system. In the future, operators can apply the measures obtained to a utilization maximization problem that finds the optimal number of OVSF codes in a Node-B to gain the maximum profit with a specific QoS constraint. The model should be useful for constructing WCDMA networks.

## References


[1] F. Adachi, M. Sawahashi, and H. Suda, "Wideband CDMA for next generation mobile communications systems," *IEEE Commun. Mag.*, vol. 36, no. 9, pp. 56-69, Sep. 1998.

[2] *3GPP Technical Specification 25.213, v5.1.0, Spreading and modulation (FDD) (Release 5)*, June 2002.

[3] E. H. Dinan and B. Jabbari, "Spreading codes for direct sequence CDMA and wideband CDMA cellular networks," *IEEE Commun. Mag.*, pp. 48-54, Sep. 1998.

[4] S. J. Lee, H.W. Lee, and D. K. Sung, "Capacities of single-code and multicode DS-CDMA systems accommodating multiclass services," *IEEE Trans. on Vehicular Tech.*, vol. 48, no. 2, pp. 376-384, Mar. 1999.

[5] S. Ramakrishna and J. M. Holtzman, "A comparison between single code and multiple code transmission schemes in a CDMA system," in *Proc. of IEEE VTC'98*, pp. 791-795, May 1998.

[6] C.-S. Wan, W.-K. Shih, and R.-C. Chang, "Fast dynamic code assignment in next generation wireless access networks," *Computer Commun.*, vol. 26, pp. 1634-1643, 2003.

[7] L.-H. Yen and M.-C. Tsou, "An OVSF code assignment scheme utilizing multiple RAKE combiners for W-CDMA," *Computer Commun.*, vol. 27, pp. 1617-1623, 2004.

[8] Y. Yang and T. P. Yum, "Maximally flexible assignment of orthogonal variable spreading factor codes for multirate traffic," *IEEE Trans. on Wireless Commun.*, vol. 3, no. 3, pp. 781-792, May 2004.

[9] A. N. Rouskas, D. N. Skoutas, G. T. Kormentzas, and D. D. Vergados, "Code reservation schemes at the forward link in WCDMA," *Computer Commun.*, vol. 27, no. 9, pp. 792-800, 2004.

[10] C. Chao, Y. Tseng, and L. Wang, "Reducing internal and external fragmentations of OVSF codes in WCDMA systems with multiple codes," in *Proc. of IEEE WCNC'03*, pp. 693-698, 2003.

[11] T. Minn and K. Y. Siu, "Dynamic assignment of orthogonal variable-spreading-factor codes in W-CDMA," *IEEE Journal on Selected Areas in Commun.*, vol. 18, no. 8, pp. 1429-1440, Aug. 2000.

[12] R. G. Cheng and P. Lin, "OVSF code channel assignment for IMT-2000," in *Proc. of IEEE VTC'00*, pp. 2188-2192, 2000.

[13] T. Ottosson and T. Palenius, "The impact of using multicode transmission in the WCDMA system," in *Proc. of IEEE VTC'99*, vol. 2, pp. 1550-1554, May 1999.

[14] M. V. Cromie, M. L. Chaudhry, and W. K. Grassmann, "Further results for the queueing system $M^X/M/c$," *Journal of the Operational Research Society*, vol. 30, no. 8, pp. 755-763, 1979.